



Research Paper / Makale

Origin of Barite Mineralization in the Doğanşehir (Malatya): Trace and Rare Earth Element, Isotope and Fluid Inclusion Evidence

Hatice KARA^{1a}, Dicle BAL AKKOCA^{1b}

¹Fırat University, Department of Geological Engineering, 23119, Elazığ, Turkey
haticekara@firat.edu.tr

Received/Geliş: 06.04.2021

Accepted/Kabul: 25.05.2021

Abstract: This study the main objective presented the geochemical and isotopic characteristics of the barite mineralization at the Doğanşehir (Malatya), located in the Eastern Taurids. These mineralizations observed are included in crack zones of metamorphic rocks. Trace element data of barite in the study area show that Ba, Pb and Zn may have been derived from different sources: these elements come from recrystallized limestones and siliceous rocks. The trends of the REE and the plots of the values of barites on the Ce_N/Sm_N versus Ce_N/Yb_N diagram indicate that seawater dominated the hydrothermal fluid depositing the barite and supplied the barium and sulfate ions, while a fluid mixture of seawater. Pb isotope studies ($^{206}Pb/^{204}Pb=17.04-19.2$; $^{207}Pb/^{204}Pb=14.33-17.00$ and $^{208}Pb/^{204}Pb=34.19-41.66$) indicate that the lead in barite was derived from the mantle, orogen, and crust and was slightly contaminated by the basement rocks. Sulfur isotopic studies indicate that the sulfur in barite has been derived from seawater sulfate sources ($\delta^{34}SVCDT$ values range from 17.5 ‰ to 30.7 ‰). Microthermometric studies on barite samples range from 85°C to 122°C, with an average of 110°C. Salinities vary from 0.2 to 2.6 NaCl wt%. Homogenization temperatures of the studied fluid inclusions suggest which were probably formed in epithermal conditions.

Keywords: barite, lead isotope, sulphur isotope, fluid inclusion

Doğanşehir (Malatya)'da ki Barit Cevherleşmelerinin Kökeni: İz ve Nadir Toprak Element, İzotop ve Sıvı Kapanım Bulguları

Öz: Bu çalışmada, Doğu Toroslar'da yer alan Doğanşehir (Malatya) barit cevherleşmesinin jeokimyasal ve izotopik özellikleri ortaya konmuştur. Gözlenen bu cevherleşmeler metamorfik kayaların çatlak zonları içinde yer almaktadır. Çalışma alanındaki baritlerin eser element verileri, Ba, Pb ve Zn'nin farklı kaynaklardan türetilmiş olabileceğini göstermektedir: bu elementler rekristalize kireçtaşlarından ve silisli kayalardan gelmektedir. REE ve Ce_N / Sm_N 'ye karşı Ce_N / Yb_N diyagramındaki barit değerlerinin grafikleri, deniz suyunun bariti çökelten hidrotermal sıvıya hükmettiğini ve baryum ve sülfat iyonlarını sağlarken, akışkan bir deniz suyu karışımı sağladığını göstermektedir. Pb izotop çalışmaları ($^{206}Pb / ^{204}Pb = 17.04-19.2$; $^{207}Pb / ^{204}Pb = 14.33-17.00$ ve $^{208}Pb / ^{204}Pb = 34.19-41.66$), baritteki kurşunun manto, orojen ve kabuktan türetildiğini ve taban kayaları tarafından hafifçe kirlendiğini göstermektedir. Kükürt izotopik çalışmaları, baritteki kükürtün deniz suyu sülfat kaynaklarından türetildiğini göstermektedir ($\delta^{34}SVCDT$ değerleri 17,5 ‰ ila 30,7 ‰ arasındadır). Barit örneklerinde yapılan mikrotermometrik çalışmalar, 85 ° C ile 122 ° C arasında değişmekte, ortalama 110 ° C olduğu belirlenmiştir. Tuzluluklar ağırlıkça % 0,2 ila 2,6 NaCl arasında değişmektedir. İncelenen sıvı kapanımlarının homojenleşme sıcaklıkları, muhtemelen epitermal koşullarda oluşmuş olduğunu düşündürmektedir.

Anahtar Kelimeler: barit, kurşun izotop, kükürt izotop, sıvı kapanım

How to cite this article

Kara, H., Bal Akkoca, D., "Origin of Barite Mineralization in the Doğanşehir (Malatya): Trace and Rare Earth Element, Isotope and Fluid Inclusion Evidence" El-Cezeri Journal of Science and Engineering, 2021, 8 (2); 1035-1050.

Bu makaleye atıf yapmak için

Kara, H., Bal Akkoca, D., "Doğanşehir (Malatya)'da ki Barit Cevherleşmelerinin Kökeni: İz ve Nadir Toprak Element, İzotop ve Sıvı Kapanım Bulguları" El-Cezeri Fen ve Mühendislik Dergisi 2021, 8 (2); 1035-1050.
ORCID ID: *0000-0003-3441-9865; *0000-0003-3279-8443

1. Introduction

The Tauride in the Alpine - Himalayan orogenic belt, contain iron, manganese, bauxite, barite, barite±lead, barite±lead±zinc and lead±zinc deposits (Isparta, Konya, Antalya, Mersin, Adana, Malatya, Muş and Hakkari). While there are reviews of these deposits of the Tauride Belt [1-8], there are no detailed literature studies on the formation of the barite mineralization in the Doğanşehir.

Mineralizations in the Taurid Belt are generally associated with Paleozoic-Mesozoic carbonate rocks (Fig 1). According to some researchers, carbonated-hosted Taurids (e.g., Isparta, Konya, Kayseri and Antalya) majority show partial similarity to the Mississippi Valley-type [3, 5]. The Bolkardağ mineralizations in the Central Taurids Mountains are relatively close to the igneous source, while the Aladağ mineralizations are relatively remote to the igneous source, and they are defined as vessel type magmatic-hydrothermal deposits [9]. Some researcher suggested that the barite mineralizations in the Eastern Taurids (Adana-Feke) formed with hydrothermal processes [7, 10]. There is a carbonate-hosted Pb-Zn deposit in the Horzum (Adana-Turkey) province, which identified as a carbonate-replacement Pb-Zn deposit (CRD Pb-Zn) due to its higher formation temperature and higher temperature mineral paragenesis [11].

The study region is in the Doğanşehir (Malatya), located in the Eastern Taurids. There and around investigations have been performed many geological, mineralogical and petrographic [12-20]. Barite and Ba±Pb±Zn mineralizations in this region are hosted by limestone and volcanic and along with the contact of these volcanics with metamorphics, it is suggested that mineralizations have hydrothermal source-related with volcanic [12, 21, 22]. The current research presents the geochemical characteristics of the barite mineralization at the Doğanşehir (Malatya). It also presents a description of the physicochemical conditions of fluid inclusion in barite minerals. The main objective is to determine the geochemical features of barite in the Doğanşehir area.

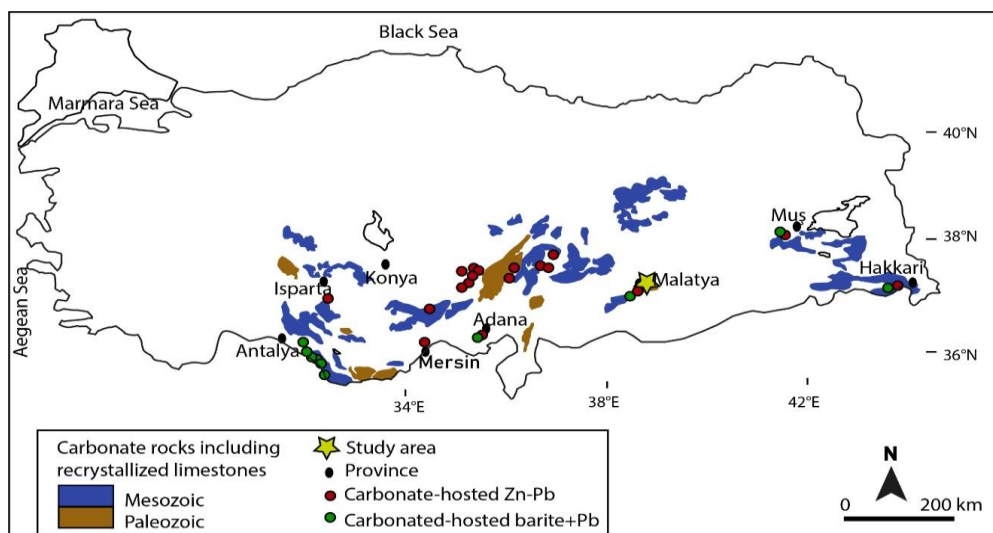


Figure 1. Distribution of the carbonate-hosted Ba±Pb±Zn districts of Turkey with on host-rock lithology [23, 24].

2. Experimental Methods

2.1. Materials and Methods

Samples were collected from barite and host rocks in the study area. Representative samples of barite and host rocks were analysed for their rare earth and trace element compositions. Acidic

dissolution and filtering processes were carried out at Bureau Veritas Minerals (BVM) Laboratories (Canada). Rare earth and trace element analyses were made using inductively coupled plasma mass spectrometry (ICP-MS). High-resolution ICP-MS (HR-ICP-MS) analysis for Pb/Pb and ^{34}S isotopes of barites were conducted along with high-precision multi-element analysis at Bureau Veritas Minerals (BVM) Laboratories (Canada). Samples were weighed into tin capsules and the sulphur isotopic composition measured using a MAT 253 Stable Isotope Ratio Mass Spectrometer coupled with a Costech ECS 4010 Elemental Analyzer. The data obtained were reported in the delta (δ) notation as per mil (‰) relative to the Vienna Canyon Diablo Troilite (VCDT) international standard ($\delta^{34}\text{S}_{\text{VCDT}}$), with an analytical reproducibility of $\pm 0.2\%$. Microthermometry of the fluid inclusions of barites was carried out using a Linkam THMS 600 heating-cooling stage (Liquid Occupation and Ore Microscopy Laboratory of Pamukkale University Department-Turkey). The temperature of phase changes for eutectic melting (T_e), and ice melting (T_{mice}) and homogenization of the vapour phase (T_h) were recorded and it was determined that the measurement error is less than $\pm 0.5^\circ\text{C}$. The temperature of phase changes for eutectic melting (T_e), and ice melting (T_{mice}) and homogenization of the vapour phase (T_h) were recorded. The ice-melting temperatures were converted to salinities using the equation given by [25] while assuming that the fluid composition would be represented by the H_2O - NaCl system.

3. Geological Setting

The study area is located in the Doğanşehir district of Malatya province and the Eastern Tauride belt. From north to south, Turkey can be divided into four major tectonic units: the Pontides, the Anatolides, the Taurids and the Border Folds [26]. The Tauride Belt in southern Turkey is an Alpine Orogen comprising a pile of nappies or tectono-stratigraphic units formed during the closure of Neotethyan oceanic branches in the Eastern Mediterranean region [27, 28]. The study area is located in the Eastern Taurid Belt of Turkey (Fig. 2a). The units in the region consist of the Palaeozoic to Mesozoic, metamorphics, ophiolites, magmatics, sedimentary and volcanic rocks (Fig. 2b). Palaeozoic units associations in the eastern Taurids consist of Cambrian to Permian passive margin sedimentary rocks. These rocks have undergone low-grade metamorphism, and therefore the primary rock structures are still recognizable.

The units in the study area in order of age are Malatya Metamorphics (Permo-Carboniferous), Berite Group (Upper Cretaceous), Granitoids (Upper Cretaceous), Volcanics (Neogene?), Alluviums and slope debris (Plio-Quaternary). The Permo - Carboniferous Malatya Metamorphites [21, 22], which are mainly composed of recrystallized limestone, are located in the region. They are found intercalated with schists (mica-schist, quartz-sericite schist etc.) [12, 21]. Recrystallized limestones are mostly grey, white and black in colour and hard, medium-thick, locally bedded massive and calcite vein in the study area. The Malatya Metamorphics was determined as Permo-Triassic according to fossil findings [29]. Volcanic rocks (Neogene?) in the study area crop out in a narrow area [12]. The metamorphic and the volcanic rocks are the main units of the study region (Fig. 2c). In the Eastern Tauride region, there are important carbonate-hosted $\text{Ba}\pm\text{Pb}\pm\text{Zn}$ deposits. There are small-scale known and unknown mining in the study region. The barite mineralizations observed in the study region, Doğanşehir (Malatya), are included in crack zones of metamorphic rocks. Normal faults and strike-slip faults are observed in the study area. These faults may affect their settlement of mineralizations.

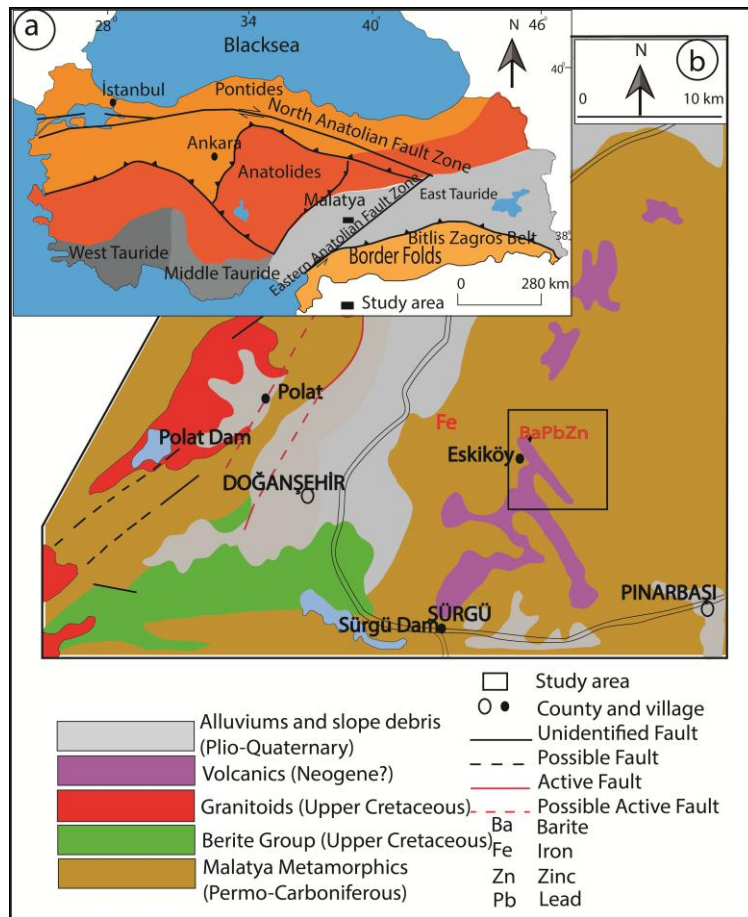


Figure 2. a) Geographic distribution of the Taurides [30]; b) Local geological map of the study region [31].

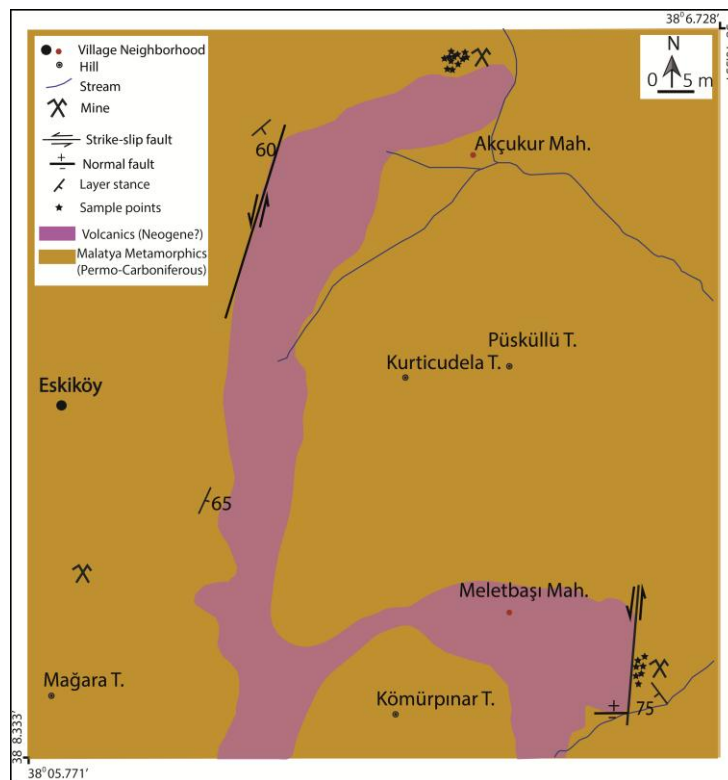


Figure 3. Simplified geological map of the Doğanşehir-Eskiköy (Malatya) (1:250000 scale).

4. Results and Discussion

4.1. Trace and Rare Earth Element Geochemistry

The trace and rare earth element compositions of both mineralized barite and recrystallized limestones samples were analyzed in this study (Table 1 and Table 2). According to the results of the analysis, the average trace element values of the samples were normalized with the average values of the Upper Crust (UC) [32]. Most of the trace element values for the barite and recrystallized limestones samples are below the detection limits of the applied method.

Table 1. Trace element (ppm) values of recrystallized limestones samples.

Sample	ES1	ES2	ES3	ES4	ES5	ES7	ES8	ES10	ES11	ES12	Average
Ba	8	666	1536	1879	237	1766	126	31	38	18	630.5
Co	-	0.9	1.3	-	0.6	-	1	0.4	-	-	0.42
Hf	0.2	-	-	-	0.3	-	0.5	-	-	-	0.1
Nb	1.7	-	0.3	-	0.7	-	1.8	0.2	1.6	-	0.63
Rb	0.8	0.2	0.6	-	5.9	-	1.1	0.2	0.2	0.2	0.92
Sr	270.5	1246.9	277.8	261.8	308.5	709.6	926.2	97	111.7	178.2	483.82
Ta	0.2	-	-	-	-	-	-	-	-	-	0.02
Th	0.8	0.2	-	-	0.7	-	0.6	-	-	-	0.23
U	2.7	0.4	0.6	0.3	3	1.8	1.1	2.3	1.6	0.4	1.42
V	16	-	9	-	13	-	-	9	9	-	5.6
Zr	12.9	2.9	1.7	0.7	9	1.7	18.3	1.4	1.1	0.8	5.05
Cu	5.9	1.8	2.7	2.2	2	-	-	-	-	-	2.48
Pb	3.1	3.2	38.4	28.5	105.4	-	-	-	-	-	2.92
Zn	19	9	374	56	104	-	-	-	-	-	35.72
As	-	-	-	-	-	-	-	-	-	-	112.4
Cd	-	-	-	-	-	-	-	-	-	-	-

Table 2. Trace element (ppm) values of barite samples.

Sample	ES24	ES25	ES26	ES27	ES28	ES29	ES30	ES31	ES32	ES33	ES34	ES35	ES36	Average
Ba	>50000	>50000	>50000	>50000	>50000	>50000	2471	328	>50000	>50000	>50000	>50000	>50000	>50000
Co	-	-	-	0.6	-	-	-	-	-	-	-	-	0.8	0.7
Hf	3.2	2.9	2.7	2.8	2.9	2.5	0.1	-	2.1	2.5	2.7	1.6	1.1	2.25
Nb	0.1	-	-	0.4	-	-	0.3	-	-	-	-	-	-	0.26
Rb	-	-	-	0.3	-	0.3	-	0.3	-	-	-	-	-	0.3
Sr	30566	30939.5	31964.7	19439.2	21381.6	21363.6	1097.1	1932.2	6826.3	9338.3	7533	4727.7	5565	14821
Ta	6.6	9.2	6.6	8	6.2	6.9	-	-	5.9	7	6.4	3.5	2.3	6.23
Th	-	-	-	-	-	-	0.2	-	-	-	-	-	-	0.2
U	-	-	-	-	-	-	-	-	-	0.1	-	2.6	0.9	1.2
V	11	11	-	-	-	-	-	-	12	39	-	14	30	19.5
Zr	1.4	1.3	0.5	2.1	0.6	1.2	3.8	1.6	0.7	0.6	0.6	1.3	0.5	1.24
Cu	8.05	5.3	16.62	8.04	4.09	20.73	2.36	0.2	3.93	0.92	0.58	22.97	8.34	5.69
Pb	76.01	3.85	19.54	4.11	2.35	27.27	1.1	0.89	>10000	1074.24	172.17	>10000	>10000	7.85
Zn	4080.9	33.3	2139.8	2548.1	914.8	3586	9.5	2.4	143.5	193.1	138.9	853.8	>10000	>10000
As	0.6	1.4	1.5	0.8	0.4	4.2	-	-	1.4	2.2	0.6	13	7.7	>10000
Cd	17.47	0.08	9.76	8.73	2.22	21.67	0.07	0.04	1.82	1.9	0.02	2.93	106.25	3.07

Trace elements of both barite and recrystallized limestones samples in the study region were normalized to the upper crust (Fig. 4). In the study area, both of the recrystallized limestones and barites are enriched in Ba, Sr, Pb and Zn, relative to UC. In this study, Ba, Pb and Zn come from may have been derived from different sources: these elements probably come from recrystallized limestones and volcanic rocks in the study region. The relatively high Sr concentration in the barite sample probably indicates an origin of the Doğanşehir barite mineralization from a low-temperature hydrothermal solution [35, 36].

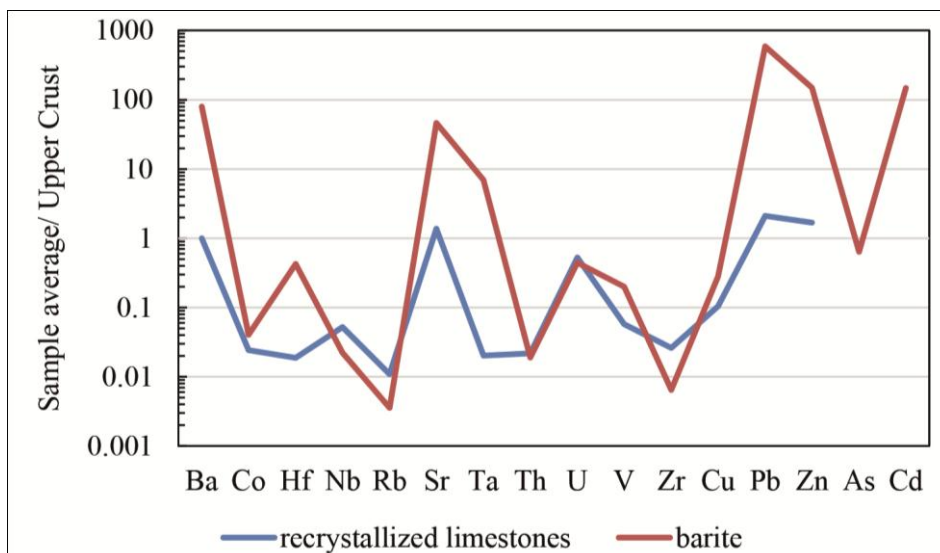


Figure 4. Normalized to the upper crust patterns of the recrystallized limestones samples in the study area. Upper crust data for normalization are from [32].

According to the results of the analysis, the rare earth element (REE) values of the samples were normalized with values of the chondrite (Table 3 and Table 4). Total REE concentrations have (1.3-119.4 ppm, n=10) in the recrystallized limestones and (5.99-88.53 ppm, n=13) in the barite. $\Sigma\text{LREE}/\Sigma\text{HREE}$ (ratios of the recrystallized limestones and barite are 3.94-13.90 and 0.42-3.79, respectively. Chondrite data for normalisation are from McDonough and Sun (1995).

Table 3. Rare earth element (ppm) values of recrystallized limestones samples

Sample	ES1	ES2	ES3	ES4	ES5	ES7	ES8	ES10	ES11	ES12	Average
La	10.1	1.5	1.5	0.9	6.1	0.6	7.1	0.6	0.4	0.9	5.18
Ce	4.9	3.1	1.2	0.8	12.6	0.7	13.3	0.5	0.7	0.6	8.96
Pr	1.8	0.37	0.25	0.12	1.55	0.05	1.66	0.05	0.05	0.08	1.16
Nd	7.7	1.4	1.1	0.5	6.3	-	7	-	-	-	7.13
Sm	1.11	0.32	0.22	0.11	1.28	-	1.17	-	-	-	1.41
Eu	0.22	0.27	0.06	0.05	0.26	0.04	0.12	-	-	-	0.27
Gd	0.99	0.46	0.38	0.19	1.16	0.09	1.1	0.09	0.08	0.07	0.95
Tb	0.09	0.07	0.05	0.02	0.16	-	0.15	-	-	0.01	0.17
Dy	0.48	0.41	0.32	0.16	0.94	0.05	0.75	0.05	0.06	0.06	0.73
Ho	0.1	0.1	0.08	0.04	0.16	-	0.15	-	-	-	0.21
Er	0.25	0.22	0.21	0.13	0.47	-	0.41	0.04	-	0.04	0.45
Tm	0.03	0.03	0.03	0.02	0.06	-	0.05	-	-	-	0.08
Yb	0.23	0.12	0.13	0.09	0.39	-	0.32	0.05	-	-	0.4
Lu	0.04	0.02	0.02	0.01	0.05	-	0.05	-	-	-	0.06
ΣREE	28.04	8.39	5.55	3.14	31.48	1.53	33.33	1.38	1.29	1.76	23.91
$\Sigma\text{LREE}/\Sigma\text{HREE}$	11.74	4.97	3.94	4.13	8.26	13.9	10.47	5.75	11.5	7.9	8.15

Table 4. Rare earth element (ppm) values of barite samples.

Sample	ES24	ES25	ES26	ES27	ES28	ES29	ES30	ES31	ES32	ES33	ES34	ES35	ES36	Average
La	2	1.8	1.7	2.2	1.9	1.6	3.4	6.6	2.1	2	2.5	2.3	1.7	2.45
Ce	0.7	0.5	0.3	0	0.2	0.3	13.9	24.5	0.2	0.1	0.2	0.1	0.4	3.18
Pr	0.06	0.05	0	0.05	0	0.03	2.63	4.27	0	0	0	0.04	0.03	0.55
Nd	-	-	-	-	-	-	15.2	23.3	-	-	-	-	-	19.25
Sm	0.78	0.66	0.63	0.61	0.45	0.48	5.37	8.06	0.47	-	-	0.41	0.35	1.66
Eu	-	-	-	-	-	-	2	3.31	-	-	-	-	-	0.41
Gd	5.63	3.81	3.65	4	3.86	3.73	5.67	7.67	3.34	2.93	3.37	2.42	2.31	3.74
Tb	0.04	0.03	0.03	0.07	0.04	0.05	0.82	1.02	0.05	0.06	0.07	0.04	0.04	0.18
Dy	0.47	0.79	0.81	1.07	1.07	1.16	4.31	5.24	1.6	1.92	2.6	1.04	1	1.78
Ho	-	-	-	-	-	-	0.76	0.86	-	-	-	-	-	0.81
Er	-	-	-	-	-	-	1.78	2.11	-	-	-	-	0.03	1.31
Tm	0.02	0.02	0.01	0.01	-	0.02	0.22	0.22	0.01	0.02	0.01	0.01	0.02	0.05
Yb	0.2	0.12	0.13	0.16	0.13	0.12	1.25	1.22	0.07	0.11	0.09	0.06	0.1	0.29
Lu	0.02	0.02	0.01	0.01	0.01	0.02	0.16	0.15	-	0.01	-	-	0.01	0.04
Σ REE	9.92	7.8	7.27	8.18	7.66	7.51	57.47	88.53	7.84	7.15	8.84	6.42	5.99	17.74
Σ LREE														
Σ HREE														
Σ LREE/ Σ HREE	0.55	0.63	0.57	0.54	0.5	0.47	2.84	3.79	0.55	0.42	0.44	0.8	0.71	1.62
Ce _N /Sm _N	0.21	0.17	0.11	-	0.10	0.14	0.60	0.71	0.10	-	-	0.05	0.26	
Ce _N /Yb _N	0.87	0.98	1.17	-	0.38	0.62	2.79	5.04	0.71	0.22	0.55	0.41	1.01	
Ce/Ce*	0.48	0.40	-	-	-	0.33	1.11	1.10	-	-	-	0.07	0.42	

The REE concentrations of the Doğanşehir barite mineralization (Table 4), normalised using the chondrite abundances of [37], show the total REE (Σ REE), varying from 5.99 to 88.53 ppm, with a mean of 17.74 ppm. Rare earth elements normalized to chondrites, the trends of the REE are characterized by generally low concentrations of REE, with the except for Eu (Fig. 5). As such, the results may represent a mixture of multiple, including seawater, hydrothermal fluids and terrigenous input [38]. Ce/Ce* values of recrystallized limestones and barite are between 0.84 and 0.63 respectively in this study (Table 4). The results may represent mixtures of multiple types by including seawater and hydrothermal fluids [39]. Besides, the distribution of normalised values on the Ce_N/Sm_N versus Ce_N/Yb_N diagram indicate that seawater dominated the hydrothermal fluid depositing the barite and supplied the barium and sulfate ions, while a fluid mixture of seawater (Fig. 6).

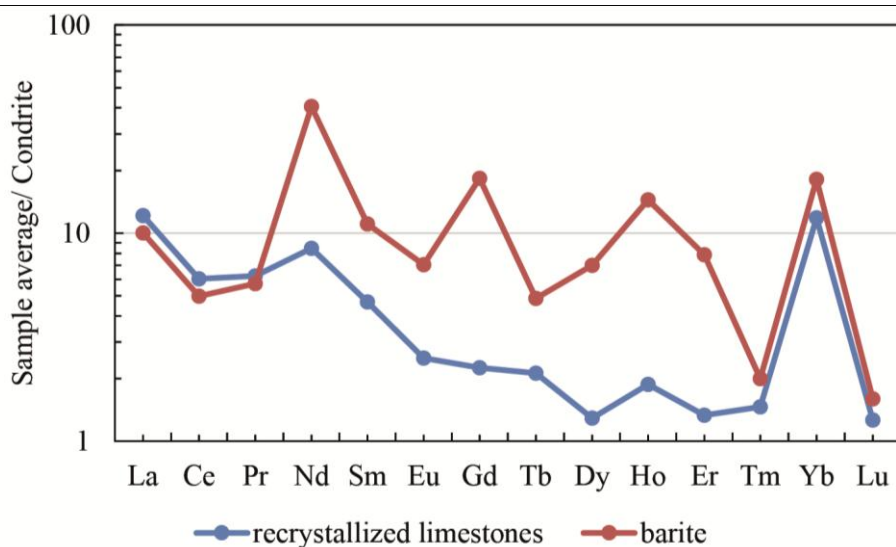


Figure 5. Chondrite normalised REE patterns of the Doğanşehir barite mineralization. Chondrite data for normalization are from [37].

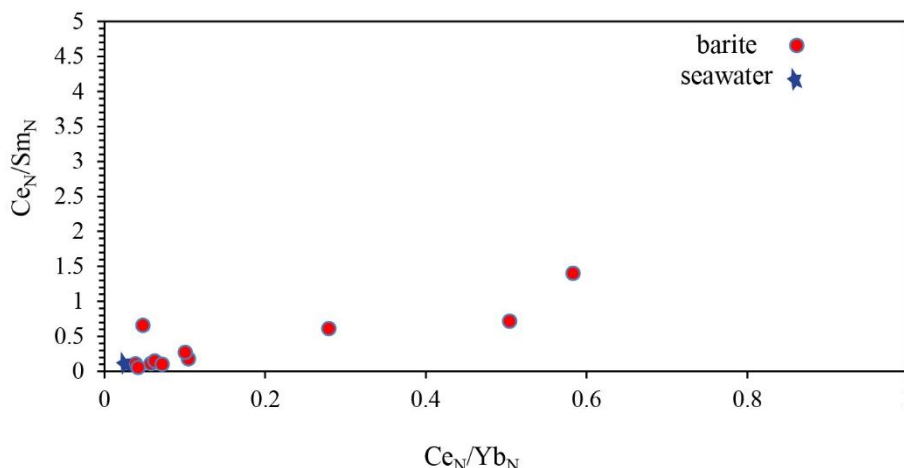


Figure 6. The plot of the values of barites on the Ce_N/Sm_N versus Ce_N/Yb_N diagram [39].

4.2. Microthermometry of Fluid Inclusions

Fluid inclusions were studied in five selected barite samples that had been collected from the barite mineralized main vein and one of the barite veinlets. The initial melting (T_{FM}), final melting (T_{mICE}), and homogenization (T_H) of the samples are shown in Table 5. T_{FM} and T_{mICE} data have been interpreted by using the tables [25, 33]. Primary and secondary fluid inclusions in barite were determined using the criteria of [34].

Table 5. Microthermometric data of fluid inclusions in barite samples.

Primary inclusion		
T_{FM}	T_{ICE}	T_H (°C)
-55	-0.1	88
-55	-0.2	85
-55	-0.4	110
-55		115
-55	-1.5	118
-55	-0.4	110
-55	-1	120
-55	-1	122
-55	-1.3	120
-55	-0.1	120
-55	-0.7	120
-55	-0.4	100

The inclusions can be divided into three groups: 1) two-phase liquid-vapour (liquid-rich); 2) monophasic (only liquid phase) and 3) monophasic (only vapour phase). Primary and pseudo secondary inclusions are consistently simple two-phase liquid-vapour types with no daughter mineral or separated CO₂ phase at room temperature. Primary fluid inclusions are interpreted as representing the fluids present at the time of hydrothermal mineral growth. These primary fluid inclusions define by trapping during crystal growth, while the secondary inclusions occur as fracture-controlled arrays after the growth of the host crystal [34, 40]. The vast majority of primary inclusions form single-phase (liquid) inclusions and have fewer two-phase (liquid+vapour)

inclusions (Fig. 7a and 7b). These inclusions are found in sizes ranging from 3 microns to 40 microns and are generally rounded ellipsoidal and irregular shapes. Fluid inclusion studies were mostly done on small and round inclusions as recommended by [41] to minimize the effects of probable stretching of fluid inclusions during heating measurements in barite. According to the petrographic investigations, barite minerals were formed at the earliest stage of mineralization and were followed by sulfide minerals and quartz crystallization. In this context, it was assumed that primary inclusions in barite represent the barite-forming fluid.

The values of T_H measured for 11 fluid inclusions of the barite samples studied range from 85°C to 122°C (Fig.8a), with an average of 110°C. The values of T_{mICE} varied from -1.5°C to -0.1°C, with an average of -10.9°C. The salinity of fluid inclusions (in wt% NaCl eq.) was estimated from the TLM data using the equation of [25]. The TLM data yield fluid salinities ranging from 0.2 to 2.6 wt% NaCl eq. (Fig.8b), with an average of 1.5 wt% NaCl eq. The values of TFM measured at -55.0°C. This measured temperature value indicates that salts such as NaCl, CaCl₂, and MgCl₂ are present in the solution, as compared to the eutectic temperatures of various water-salt systems.

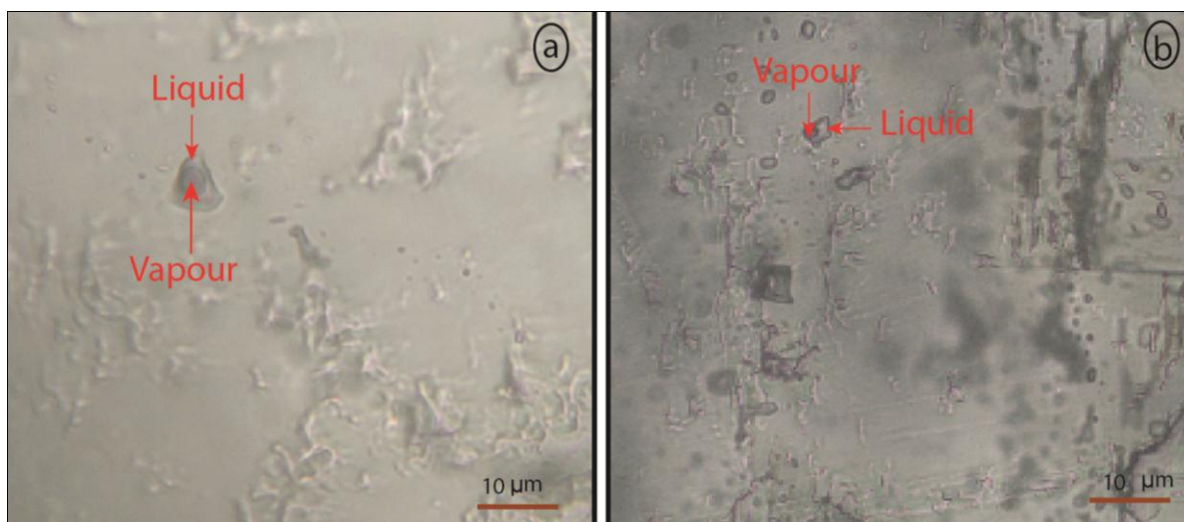


Figure 7. Types of fluid inclusions within the barite crystals studied. a) Two-phase (liquid/vapour) inclusions (No:ES-32); b) Two-phase vapour, liquid-rich (No:ES-31).

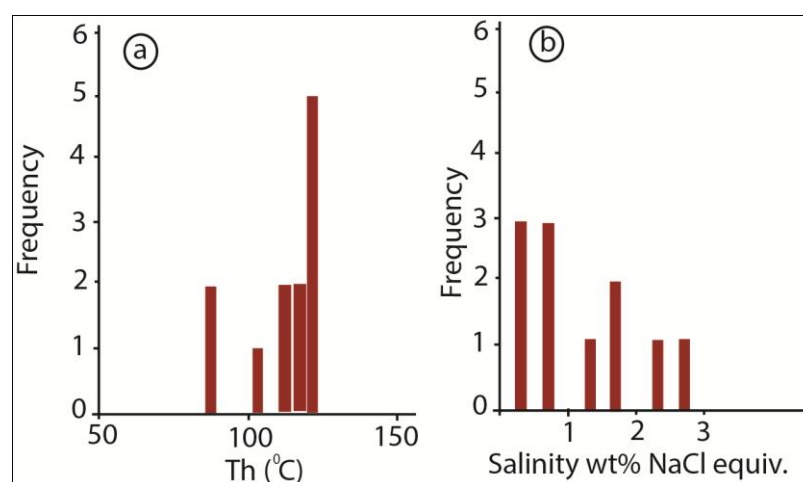


Figure 8. a) Homogenization temperature (T_H) versus frequency histogram, b) Frequency versus wt. % NaCl equivalent salinity histogram in barite in the Doğanşehir (Malatya).

When the relationship between salinity and homogenization temperature is considered, it is observed that the salinity (2.6 %NaCl) of the solutions and the temperature (122°C) is low during the formation of barites. The homogenization temperature and % NaCl equivalent salinity values in this study were compared with the data obtained in similar deposit types. Homogenization temperatures of the studied fluid inclusions suggest which were probably formed in epithermal conditions (Fig. 9). Epithermal deposits are primarily formed from modified, surface-derived fluids that have circulated to a range of depths within the fragile regime of the crust, usually in the field of elevated crustal permeability and heat flow. They are therefore typified by low salinity fluids and a range of homogenization temperatures [42].

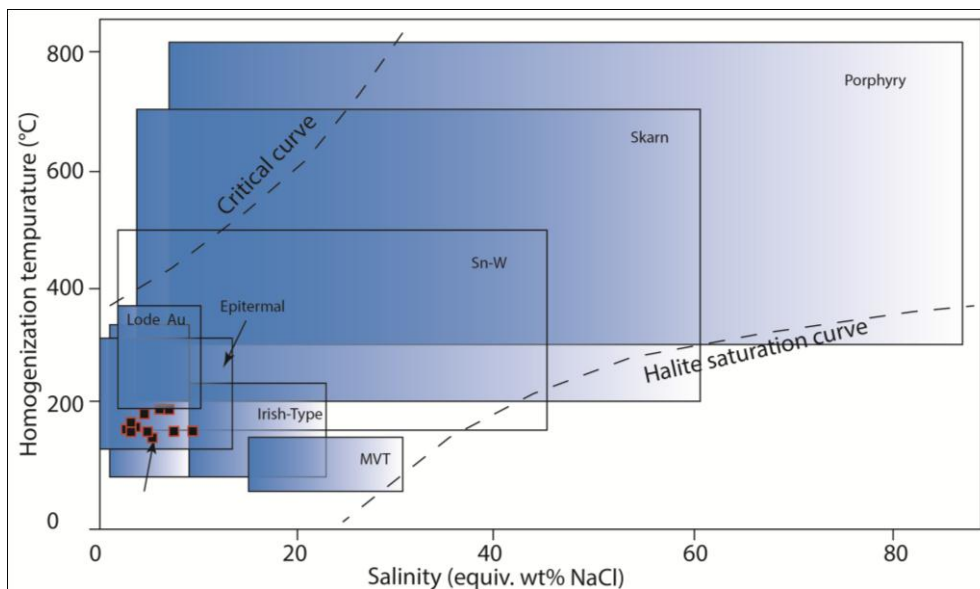


Figure 9. T_H plot of homogenization temperature vs. salinity [42].

4.3. Pb and S Isotopes

The Pb and S isotopes compositions in barite samples taken from Doğanşehir (Malatya) are presented in Table 6 and Table 7, respectively. The Pb isotope compositions of the study region barite are $^{206}\text{Pb}/^{204}\text{Pb}$, $^{207}\text{Pb}/^{204}\text{Pb}$, and $^{208}\text{Pb}/^{204}\text{Pb}$ ratios ranging from 17.04 to 19.2, from 14.33 to 17.00, and from 34.19 to 41.66, respectively. The $\delta^{34}\text{S}_{\text{VCDT}}$ values of sulfide samples range from +17.5 to +30.7‰.

Pb isotopes can be used to help decipher the genesis of mineralization and the origin of lead [43]. According to the plumbotectonic model of Zartman and Doe (1981), Pb isotope values were plotted above the orogene curve in the thorogenic ($^{208}\text{Pb}/^{204}\text{Pb}$ vs. $^{206}\text{Pb}/^{204}\text{Pb}$) diagram. Likewise, Pb isotope values were plotted between the mantle, the orogene and the lower crust curve in the uraniumogenic ($^{207}\text{Pb}/^{204}\text{Pb}$ vs. $^{206}\text{Pb}/^{204}\text{Pb}$) diagram (Fig. 11a and 11b). Pb isotope studies indicate that the lead in barite was derived from mantle, orogen and crust sources (Fig.10). Also, Pb isotopes values indicate that they were slightly contaminated by the basement rocks.

The isotopic compositions of sulfur ($\delta^{34}\text{S}$ values) in sulfide minerals and/or mineralizing fluid ($\delta^{34}\text{S}_{\text{ΣS}}$) in the sulfide-bearing mineralizations help us understand both possible sources of sulfur and other metallogenic elements and figure out the conditions of formation of sulfides in mineralizations [44]. The $\delta^{34}\text{S}$ analysis results of the samples from the study area were investigated in order to determine the source of the sulfur contained in the barite.

Table 6. Lead isotope composition of barite samples in the Doğanşehir (Malatya)

Sample	$^{206}\text{Pb}/^{204}\text{Pb}$	$^{207}\text{Pb}/^{204}\text{Pb}$	$^{208}\text{Pb}/^{204}\text{Pb}$
ES24	17.768	15.546	36.064
ES25	19.200	17.000	39.800
ES26	18.000	15.703	37.666
ES27	16.666	14.666	36.166
ES28	18.666	17.000	41.666
ES29	17.555	15.361	35.902
ES32	18.069	15.478	38.152
ES33	17.045	14.335	36.129
ES34	16.686	14.852	34.193
ES35	18.188	15.533	36.068
ES36	18.292	15.625	38.000
ES38	18.255	15.679	38.816
ES39	18.070	15.466	37.872
ES40	17.965	15.261	37.765
ES41	17.781	15.384	37.749
ES42	17.880	15.530	38.302

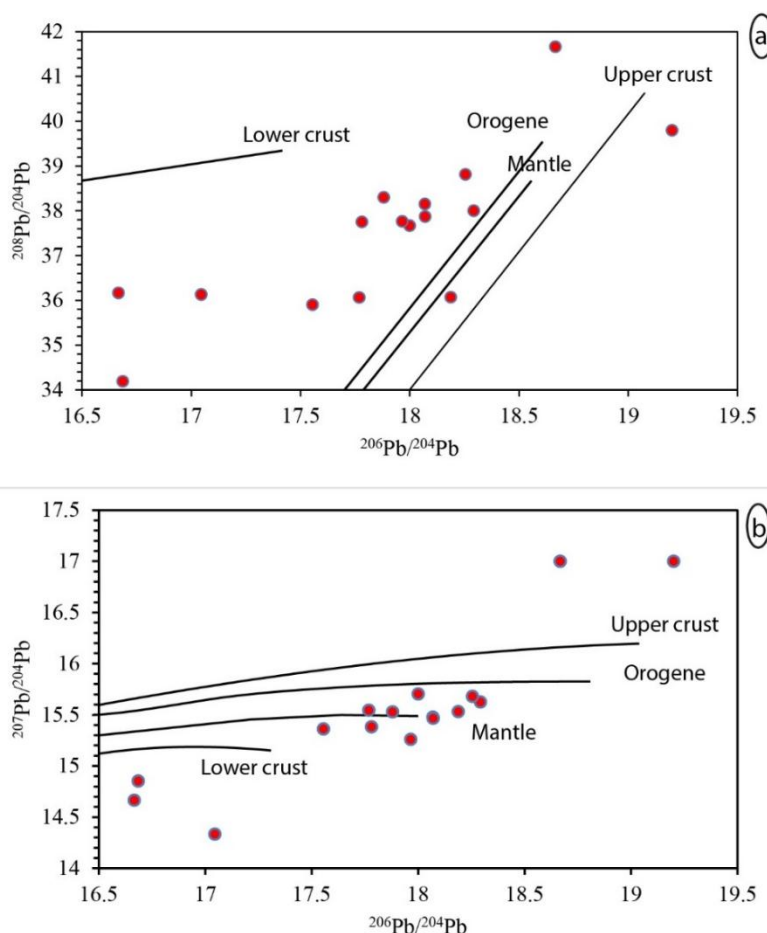


Figure 10. Plots of $^{208}\text{Pb}/^{204}\text{Pb}$ vs. $^{206}\text{Pb}/^{204}\text{Pb}$ and $^{207}\text{Pb}/^{204}\text{Pb}$ vs. $^{206}\text{Pb}/^{204}\text{Pb}$ for barite samples of the Doğanşehir (Malatya) district. Curves of growth trends for Pb isotope ratios are from the plumbotectonic model of [43].

Table 7. Sulfur isotope composition of barite samples in the Doğanşehir (Malatya).

Sample	Mineral	$\delta^{34}\text{S}$ ‰ vs VCDT
ES24	barite	30.7
ES25	barite	28
ES32	barite	22.5
ES33	barite	19.9
ES35	barite	23.4
ES36	barite	17.5

It has been compared with other barite deposits which have similar formation conditions in age and/or tectonically, showing similarities in terms of mineralogical, textural, and host rock. In this study, $\delta^{34}\text{S}$ values of barite ores range from 17.5‰ to 30.7‰ (Fig. 11). $\delta^{34}\text{S}$ values in the study region are different from those of mantle-derived magmatic sulfur (~0‰), whereas close to those of Devonian sulfate (25‰). However, they are appropriate with Cambrian to Triassic seawater sulfate (+15‰ to +35‰) [45, 46, 47].

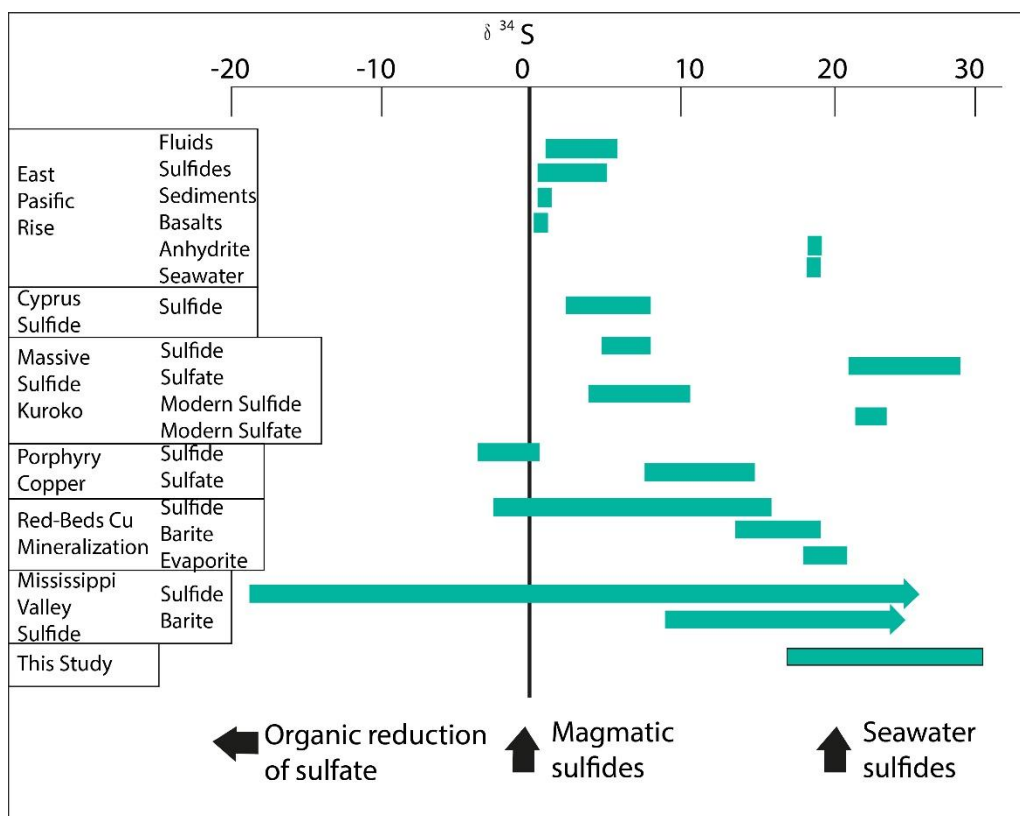


Figure 11. $\delta^{34}\text{S}$ values for sulfur-bearing minerals in this study and various deposits [48, 49, 50, 51, 52].

6. Conclusions

This study located at the Doğanşehir (Malatya), located in the Eastern Taurids. Barite mineralizations are included in crack zones of metamorphic (Permo-Triassic) rocks in the study area. Trace elements of both barite and recrystallized limestones samples in the study region were normalized to the upper crust. In the study area, both of the recrystallized limestones and barites are enriched in Ba, Sr, Pb and Zn, relative to UC. Trace element data show that Ba, Pb and Zn may have been derived from different sources: these elements probably come from recrystallized limestones and siliceous rocks in the study area.

According to the results of the analysis, the rare earth element (REE) values of the samples were normalized with values of the chondrite. Total REE concentrations have (1.3-119.4 ppm, n=10) in the recrystallized limestones and (5.99-88.53 ppm, n=13) in the barite. $\Sigma\text{LREE}/\Sigma\text{HREE}$ (ratios of the recrystallized limestones and barite are 3.94-13.90 and 0.42-3.79, respectively). Ce/Ce^* values of recrystallized limestones and barite are between 0.84 and 0.63 respectively in this study. The trends of the REE and the plots of the values of barites on the Ce_N/Sm_N versus Ce_N/Yb_N diagram indicate that seawater dominated the hydrothermal fluid depositing the barite and supplied the barium and sulfate ions, while a fluid mixture of seawater.

The microthermometric studies indicate that the vast majority of primary inclusions form single-phase (liquid) inclusions and have fewer two-phase (liquid+vapour) inclusions. The values of T_H measured for 11 fluid inclusions of the barite samples studied range from 85°C to 122°C (Fig.8a), with an average of 110°C. The values of T_{mICE} varied from -1.5°C to -0.1°C, with an average of -10.9°C, salinities ranging from 0.2 to 2.6 wt% NaCl eq., with an average of 1.5 wt% NaCl eq. The values of TFM measured at -55.0°C. When the relationship between salinity and homogenization temperature is considered, it is observed that the salinity (2.6 %NaCl) of the solutions and the temperature (122°C) is low during the formation of barites. Homogenization temperatures of the studied fluid inclusions suggest which were probably formed in epithermal conditions. Epithermal deposits are primarily formed from modified, surface-derived fluids that have circulated to a range of depths within the fragile regime of the crust, usually in the field of elevated crustal permeability and heat flow.

The Pb isotope compositions of the study region barite are $^{206}\text{Pb}/^{204}\text{Pb}$, $^{207}\text{Pb}/^{204}\text{Pb}$, and $^{208}\text{Pb}/^{204}\text{Pb}$ ratios ranging from 17.04 to 19.2, from 14.33 to 17.00, and from 34.19 to 41.66, respectively. In this study, $\delta^{34}\text{S}$ values of barite ores range from 17.5‰ to 30.7‰. Pb isotope studies indicate that the lead in barite was derived from mantle, orogen and crust sources (Fig.10). Also, Pb isotopes values indicate that they were slightly contaminated by the basement rocks. $\delta^{34}\text{S}$ values in the study region are different from those of mantle-derived magmatic sulfur (~0‰), whereas close to those of Devonian sulfate (25‰). However, they are appropriate with Cambrian to Triassic seawater sulfate (+15‰ to +35‰).

Acknowledgements

This study was supported by the Scientific Research Office of Fırat University (FUBAP), Project No. MF 16.63.

Author (s) Contributions

Field studies, sample preparation, and data evaluation were carried out together. Both authors have read and approved the final version of the article.

Conflict of Interest

The authors declare that there is no conflict of interest.

References

- [1]. Kuşçu, M., Cengiz, O., "Karbonatlı kayaçlara bağlı Orta Toroslar Zn-Pb cevherleşmelerinin kükürt izotopları incelemesi", Türkiye Jeoloji Kurultayı Bülteni, 2001, 44, 59-73.
- [2]. Gökçe, A., Bozkaya, G., "Lead and Sulfur Isotopic Studies of the Barite-Galena Deposits in the Karalar Area (Gazipasa-Antalya), Southern Turkey", Journal of Asian Earth Sciences, 2007, 30, 53-62.

- [3]. Cengiz, O., Uçurum, A., Muchez, P., "Orta Toroslar'daki Sarkikaraağaç (Isparta), Hüyük, Beyşehir (Konya) ve Gazipasa (Antalya) Barit Yataklarının Kökeninin Sıvı Kapanım ve S, O, C, Sr ve Pb izotop incelemeleri ile Belirlenmesi", Proje No: 104Y032, 2008, Ankara.
- [4]. Çiftçi, E., Demirören, S.S., "Orta Toroslar Pb-Zn Damar yataklarının kurşun izotop karakteristikleri", TUBITAK Projeno: ÇAYDAG-110Y016, 2011, Ankara.
- [5]. Hanilçi, N., Öztürk, H., "Geochemical/isotopic evolution of Pb-Zn deposits in the Central and Eastern Taurides, Turkey", *International Geology Review*, 2011 53, 1478-1507.
- [6]. Akyıldız, M., Yıldırım, N., Gören, B., "Yıldırım, E., İlhan, S., The origin of vein-type lead-zinc deposits host in Paleozoic metamorphic rocks at the Southeast Anatolian Orogenic Belt (Kupluce-Adıyaman, Southeastern Turkey)", *Journal of African Earth Sciences*, 2015, 191-202.
- [7]. Taş Özdoğan, A., Uras, Y., Öner, F., "Geochemistry of the barite deposits near Adana-Feke area (Eastern Taurides) ", *Russian Geology and Geophysics*, 2017, 1351-1367.
- [8]. Uras, Y., Yalçın, C., Özen, M., "Haraptepe (Horzum-Adana) Pb-Zn Cevherleşmesinin Kökenine Genel Bir Yaklaşım", *Çukurova Üniversitesi Mühendislik Mimarlık Fakültesi Dergisi*, 2020, 35(4), 873-882.
- [9]. Koptagel, O., Ulusoy, U., Efe, A., "A study of sulphur isotopes in determining the genesis of Goynuk and Celalaga Desandre Pb-Zn deposits, eastern Yahyali, Kayseri, Central Turkey", *Journal of Asian Earth Sciences*, 2005, 25, 279-289.
- [10]. Uras, Y., Öner, F., Yaman, S., "Geochemie des Fluoritvorkommens von Feke (Adana-Türkei) im Osten des Taurusgebirges: Geochemistry of fluorite occurrence from Feke (Adana-Turkey) in the East Taurid Mountains", *Geochemistry*, 2003, 55-62.
- [11]. Hanilçi, N., Öztürk, H., Kasapçı, C., "Carbonate-Hosted Pb-Zn Deposits of Turkey, Mineral Resources of Turkey", *Modern Approaches in Solid Earth Sciences*, 2019, 16, (10), 497-533
- [12]. Sağiroğlu, A., "Cafana (Görgü) Malatya carbonated Pb - Zn deposits", *Cumhuriyet University Engineering Faculty Journal, Serie A- Earth Sciences*, 1988, 3-13.
- [13]. Önal, A., "Polat-Beğre (Doğanşehir) çevresindeki magmatik kayaların petrografik ve petrolojik özellikleri", *Fırat Üniversitesi Fen Bilimleri Enstitüsü Doktora Tezi Jeoloji Mühendisliği Anabilim Dalı, Elazığ*, 1995, 159.
- [14]. Önal, A., Altunbey, M., "Dedeyazı-Çavuşlu (Doğanşehir-Malatya) yöresindeki skarn oluşumlar ve ilişkili demir cevherleşmeleri", *Türkiye Jeoloji Bülteni*, Ankara, 1999, 1,15-27.
- [15]. Kalender, L., Kırat, G., Bölücek, C., "Sağiroğlu, A., Görgü (Malatya-Türkiye) Pb-Zn yatağının eski imalat pasalarının jeokimyası", *Türkiye Jeoloji Bülteni*, Ankara, 2009, 2,239-255.
- [16]. Sağiroğlu, A., Kara, H., Kürüm, S., "Mineralogy and geochemistry of the hematite muscovite schists of Malatya, Turkey: Could it be the first known Banded Iron Formation (BIF) in the Taurids and Anatolia? " *Carpathian Journal of Earth and Environmental Sciences*, 2013,8, 49-58.
- [17]. Özkan, A. M., "The Sedimentological and Paleontological Features of Lutetian-aged Yeşilyurt Group at the Yeşilyurt - Gündüzbey Area (Malatya, Turkey)" *El-Cezerî Journal of Science and Engineering*, 2016, 3, 372-384.
- [18]. Kırat, G., Bölücek, C., "Bioaccumulator characteristics for Pb-Zn of *Prunus Armeniaca* L. Plant (Yeşilyurt-Görgü), Turkey", *Engineering Sciences*, 2018, 13,53-63.
- [19]. Kara, H., Sağiroğlu, A., "Keban ve Malatya Metamorfitleri'ne ait organik madde içeren kayaların iz ve nadir toprak element jeokimyası", *Fırat Üniversitesi Fen Bilimleri Dergisi*, 2018, 30,1-10.
- [20]. Ertürk, M.A., Beyarslan, M., Chung, S.L., Lin, T.H., "Eocene magmatism (Maden Complex) in the Southeast Anatolian Orogenic Belt: Magma genesis and tectonic implications", *Geoscience Frontiers*, 2018, 9, 1829-1847.
- [21]. Önal, M., Tuzcu, N., Helvacı, C., "Geological setting, mineralogy and origin of the Cafana (Malatya) Zn-Pb sulfide and carbonate deposit, E Anatolia, Turkey", in *Int. Earth Sci.*

- Congress on Aegean Regions, Proceedings, ed: M. Y. Savasçın and A. H. Eronat, Izmir, D. E. University, 1990, 1, 52-58.
- [22]. Cengiz, O., Cengiz, O., "Çarıksaraylar (Şarkikaraağaç-Isparta) Kuzeyinin Jeolojisi ve Kurşunlu Barit Yatakları", Akdeniz Üniversitesi, Fen Bilimleri Enstitüsü, Yüksek Lisans Tezi, Isparta, 1991, 75.
- [23]. Yiğit, Ö., "Mineral deposits of Turkey in relation to Tethyan metallogeny: implications for future mineral exploration", *Economic Geology*, 2009, 104, 19–51.
- [24]. Santaro, L., Boni, M., Herrington, R., Clegg, A., "The Hakkari nonsulfide Zn–Pb deposit in the context of other nonsulfide Zn–Pb deposits in the Tethyan Metallogenic Belt of Turkey", *Ore Geology Reviews*, 2013, 53, 244–260.
- [25]. Bodnar, R. J., "Revised equation and table for determining the freezing point depression of H₂O–NaCl solutions", *Geochimica et Cosmochimica Acta*, 1993, 57, 683-684.
- [26]. Ketin, İ., "Anadolu'nun Tektonik Birlikleri", *MTA Dergisi*, 1966, 66, 20-34.
- [27]. Şengör, A.M.C., Yılmaz, Y., "Tethyan evolution of Turkey: a plate tectonic approach", *Tectonophysics*, 1981, 75, 181-241.
- [28]. Göncüoğlu, M.C., Dirik, K., Kozlu, H., "General characteristics of pre-Alpine and Alpine Terranes in Turkey: explanatory notes to the terrane map of Turkey", *Ann. Geol. Pays Hellen*, 1997, 37, 515-536.
- [29]. Kipman, E., "Keban'ın jeolojisi ve Keban şarियajı", *İstanbul Üniversitesi Yerbilimleri Dergisi*, 1981, 1(2), 75-81.
- [30]. Özgül, N., "Stratigraphy and Tectonic Evolution of the Central Taurides", Tekeli, O., Göncüoğlu, M.C. (eds.), *Geology of the Taurus Belt*, 1984, 77-90.
- [31]. MTA. 1/500.000 ölçekli Türkiye Jeoloji Haritası, Maden Tetkik ve Arama Genel Müdürlüğü, 2002, Ankara-Türkiye.
- [32]. Wedepohl, K.H., "The composition of the continental crust", *Geochimica et Cosmochimica Acta*, 1995, 59, 1217-1239.
- [33]. Shepherd, T.J., Ranklin, A.H., Alderton, D.H.M., "A practical guide to fluid inclusion studies", Glasgow, Blackie, New York, 1985, 239.
- [34]. Roedder, E., "Fluid Inclusions. Mineralogical Society of America", *Review in Mineralogy*, 1984, 12, 644.
- [35]. Kato, Y., Nakamura, K., "Origin and global tectonic significance of early Archean cherts from the Marble Bar greenstone belt, Pilbara Craton, Western Australia", *Precambrian Research*, 2003, 191–243.
- [36]. Jurković, I., Garašić, V., Hrvatović, H., "Geochemical characteristics of barite occurrences in the Palaeozoic complex of southeastern Bosnia and their relationship to the barite deposits of the mid-Bosnian Schist Mountain", *Geologia Croatica*, 2010, 63, 241–258.
- [37]. McDonough, W.F., Sun, S.S., "The Composition of the Earth", *Chemical Geology*, 1995, 223-253.
- [38]. Han, S., Hu, K., Cao, J., Pan, J., Xia, F., Wu, W., "Origin of early Cambrian black-shale-hosted barite deposits in South China: Mineralogical and geochemical studies", *Journal of Asian Earth Science*, 2015, 106, 79-96.
- [39]. Guichard, F., Church, T., Treuil, M., Jaffrezic, H., "Rare earths in barites: Distribution and effects on aqueous partitioning", *Geochimica et Cosmochimica Acta*, 1979, 983-997.
- [40]. Van den Kerkhof, A.M., Hein, U., "Fluid inclusion petrography", *Lithos*, 2001, 55, 27-47.
- [41]. Ulrich, M.R., Bodnar, R.J., "Systematics of stretching of fluid inclusions II. Barite at 1atm. confining pressure", *Econ. Geol.*, 1988, 83, 1037-1046.
- [42]. Wilkinson, J.J., "Fluid inclusions in hydrothermal ore deposits", *Lithos*, 2001, 55, 229-272.
- [43]. Zartman, R.E., Doe, B.R., "Plumbotectonics the Model", *Tectonophysics*, 1981, 75, 135-162.
- [44]. Ohmoto, H., Goldhaber, M.B., Sulfur and carbon isotopes. *Geochemistry of hydrothermal ore deposits*, John Wiley, New York, 1997, 517-611.

- [45]. Chaussidon, M., Albarède, F., Sheppard, S.M.F., "Sulfur isotope variations in the mantle from ion microprobe analyses of micro-sulphide inclusions", *Earth Planet. Sci. Lett.*, 1989, 92,144–156.
- [46]. Zheng, Y.F., Xu, B.L., Zhou, G.T., "Geochemical studies of stable isotopes in minerals", *Earth Sci. Front.*, 2000, 7 (2), 299–320 (in Chinese with English abstract).
- [47]. Claypool, G.E., Holser, W.T., Kaplan, I.P., Sakai, H., Zak, I., "The age curves of sulfur and oxygen isotopes in marine sulfate and their mutual interpretation", *Chemical Geology*, 1980, 28, 199-260.
- [48]. Eldridge, C.S., Williams, N., Walshe, J.L., "Sulfur isotope variability in sediment-hosted massive sulfide deposits as determined using the ion microprobe SHRIMP: II. A study of the HYC deposit at McArthur River, Northern Territory, Australia", *Economic Geology*, 1993, 88,1-26.
- [49]. Rollinson, H.R., "Using Geochemical Data: Evaluation, Presentation, Interpretation, Longman, London. 1993
- [50]. Boni, M., Balassone, G., Iannace, A., "Base metal ores in the Lower Paleozoic of Southwestern Sardinia, In: Sangster, D. F.(Ed), Carbonate-hosted Lead-Zinc Deposits", *Society of Economic Geologist Special Publication*, 1996, 4,18-28.
- [51]. Hitzman, M.W., Beaty, D.W., "The Irish Zn-Pb-(Ba) orefield. In: Sangster, D.F.(Ed), Carbonate-hosted Lead-Zinc Deposits", *Society of Economic Geologists Special Publication*, 1996, 4,112-143.
- [52]. Kesler, S.E., "Appalachian Mississippi Valley-type deposits: paleoaquifers and brine provinces", In: Sangster, D.F. (Ed.), Carbonate Hosted Lead-zinc Deposits. *Society of Economic Geologists Special Publication*, 1996, 4,29–57.